Laser frequency stabilisation on a rubidium hyperfine transition

Celine Beier

Supervisors: Dr. Fritz Buchinger and Dr. Matthew Pearson

MITACS Globalink Research Internship

August 2019

Contents

1 Introduction

The collinear laser spectroscopy experiment at TRIUMF is based upon an atom or ion beam being overlapped by a counterpropagating laser beam with a frequency close to the energy of the electronic transition of interest. The atoms or ions get tuned into resonance by changing their velocity and therefore the amount the laser light gets Doppler-shifted. [1] A locking system based upon a frequency stabilised helium-neon laser (HeNe laser) ensures a stable frequency of the titanium-sapphire laser (Ti:Sap laser) used in the experiment. Both laser beams are overlapped and passed through a scanning Fabry-Perot-cavity. A Python script compares the relative position of the absorption peaks of both lasers and generates a feedback signal which stabilises the Ti:Sap laser in respect to the HeNe laser. [1] The efficiency of this system depends on the stability of the HeNe laser and in an attempt to evaluate it the Ti:Sap laser is used to create a frequency stable reference the HeNe laser can be compared to. For that purpose a locking system is required that stabilises the Ti:Sap laser on a hyperfine structure transition with an absolute fixed frequency.

The fine structure splitting describes a separation of electron energy levels with the same angular momentum but a different total angular momentum due to an interaction between the magnetic moment of the electron (linked to its spin) and the magnetic field generated by the motion of the electron relative to the nucleus. A further splitting occurs through interactions with the atomic nucleus and its magnetic moments (hyperfine structure). [2] Saturation spectroscopy allows to investigate the hyperfine structure transitions by eliminating the thermal Doppler-broadening of the spectral lines. Instead of using one light beam to excite electrons from a ground state to an excited state, two counterpropagating light beams with the same frequency are overlapped in the gas, a pump beam with a higher intensity and a lower-intensity probe beam. If the frequency is off resonance, pump and probe beam will excite gas atoms of different velocity classes due to the frequency being Doppler-shifted into different directions. On resonance, both beams excite atoms of the same velocity group and the light absorption in the probe beam lowers because the electrons are more likely to be excited by absorption of photons from the pump beam with a higher intensity. Within a Doppler-broadened absorption peak, Lamb dips appear, which either correspond to hyperfine structure transitions or are cross-over peaks occurring when several hyperfine transition are located in the same Doppler-broadened peak. In this case light

with a frequency exactly between two hyperfine transitions is both red shifted to a lower frequency correlating to one electronic transition and blue shifted to another hyperfine transition and is therefore absorbed by two different velocity groups. [3]

To generate a feedback signal for the laser that stabilises its frequency on a hyperfine transition, an additional sinusoidal modulation with a modulation frequency ν_{mod} and a modulation amplitude b is applied to the scanning laser frequency with the scanning slope a that causes changes that are small compared to the line width of the absorption peak:

$$\nu(t) = at + b\sin(\nu_{mod}t)$$

Two photodiodes are used to detect the absorption spectra of two probe beams, one of them being overlapped by a pump beam, the signals are fed into a lock-in amplifier. This input can be described by a Lorentzian function modelling the Doppler-free absorption peak

$$A(\nu) = \frac{\alpha\beta^2}{(\nu(t) - \gamma)^2 + \beta^2}$$

with the parameters α, β and γ defining the amplitude, width and centre of the Lorentzian function. If the laser drifts off resonance, the modulation causes its frequency to move periodically closer to and further away from resonance which results in an oscillation in the absorption signal detected by the photodiodes. If the laser frequency is below the resonance frequency, the oscillation of the absorption signal is in phase with the modulation, for a frequency higher than resonance the photodiode signal is 180° out of phase. The lock-in amplifier is given the modulation frequency as the reference signal which is multiplied with the photodiode signal and integrated over n oscillations:

$$o = \int_t^{t+\frac{n}{\nu_{mod}}} \frac{\alpha\beta^2}{(at + b\sin(\nu_{mod}t) - \gamma)^2 + \beta^2} \sin(\nu_{mod} + \phi)\, dt$$

If the phase shift ϕ is adjusted correctly this will lead to a positive output o if the laser frequency is below resonance and a negative result for a frequency higher than resonance. If the laser frequency is on resonance, any change will cause a decrease in the absorption signal causing the photodiode signal to oscillate with twice the modulation frequency which gets integrated by the lock-in amplifier to zero. [4] The output signal from the lock-in amplifier (Fig. 1) can be send to the laser to correct small changes in frequency if the scan is centred at the zero crossing and the scan amplitude is lowered.

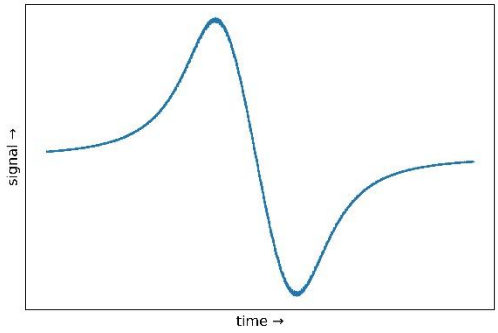

Fig. 1 Simulated output signal from the lock-in amplifier that can be used to correct small changes in the laser frequency. Due to the digital discrete integration used in this simulation small-scale irregularities show in the signal which should not appear when the integration is done analogously as by the lock-in amplifier.

In this experiment rubidium was used as a reference because as an alkali metal it has a simple atomic structure with well-known transition frequencies [5,6] which also lie within the favourable wavelength range for the used Ti:Sap laser.

2 Saturation Spectroscopy

The saturation spectroscopy setup is shown in Fig. 2. The laser beam is split into two low-intensity probe beams passing the rubidium cell and a high-intensity pump beam overlapping with one of them. A ramping voltage generated by a function generator is send to the laser control interface causing a periodic scan of a chosen frequency range.

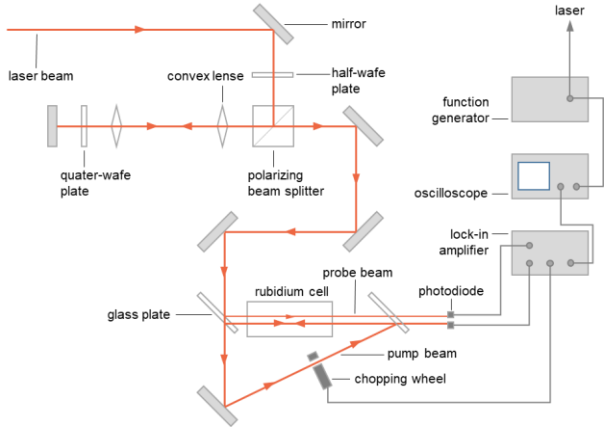

Fig. 2 Experimental setup for saturation spectroscopy.

When observed at room temperature in a vapour cell, the four Doppler-broadened absorption peaks for the D_2 transitions (transitions from the $5^1S_{1/2}$ ground state to the $5^2P_{3/2}$ excited state) in the two natural rubidium isotopes ^{85}Rb and ^{87}Rb (Fig. 3 and Fig. 5) have a line width (full width at half maximum) $\Delta\nu$ of $670\text{MHz} \leq \Delta\nu \leq 930\text{MHz}$. [5,6] As expected, the Lamb dips corresponding to hyperfine transitions and cross-over absorptions appear only in the probe beam overlapped with the pump beam (Fig. 3). A lock-in amplifier is used to subtract the signals from the two photodiodes and a chopping wheel inserted in the path of the pump beam improves the resolution of the

obtained signal (Fig. 4) and enables an identification of the transition and cross-over peaks (Fig. 5 and Fig. 6).

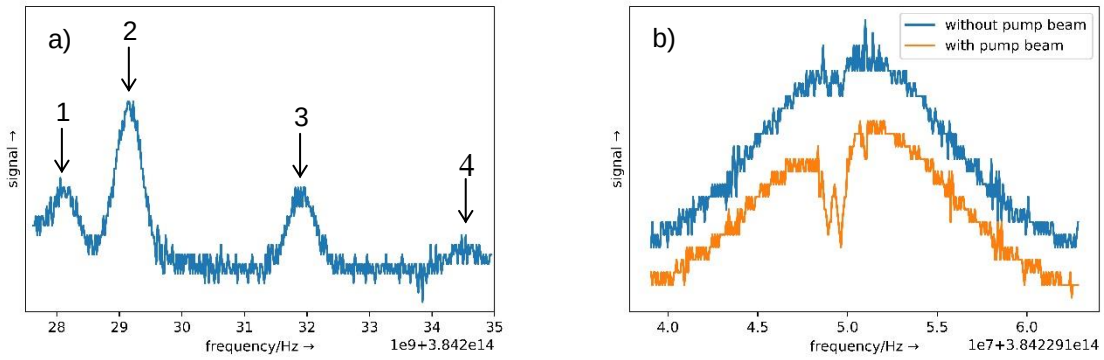

Fig. 3 a) Doppler-broadened absorption peaks of the D_2-transitions for ^{85}Rb and ^{87}Rb. **1** ^{87}Rb, F_i=2. **2** ^{85}Rb, F_i=3. **3** ^{85}Rb, F_i=2. **4** ^{87}Rb, F_i=1. b) Absorption spectra detected by the two photodiodes for probe beams with an overlapped pump beam and without. Small Lamb dips in the normal absorption spectrum are caused by alignment inaccuracies.

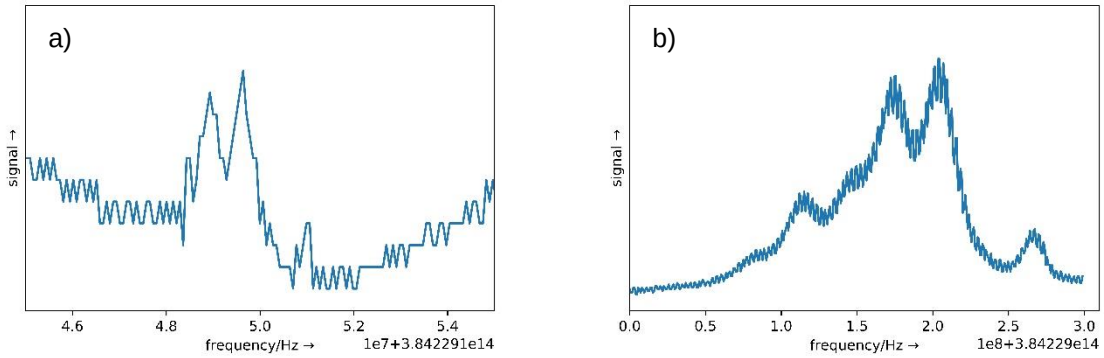

Fig. 4 Output of the lock-in amplifier a) before and b) after a chopping wheel was installed in the setup.

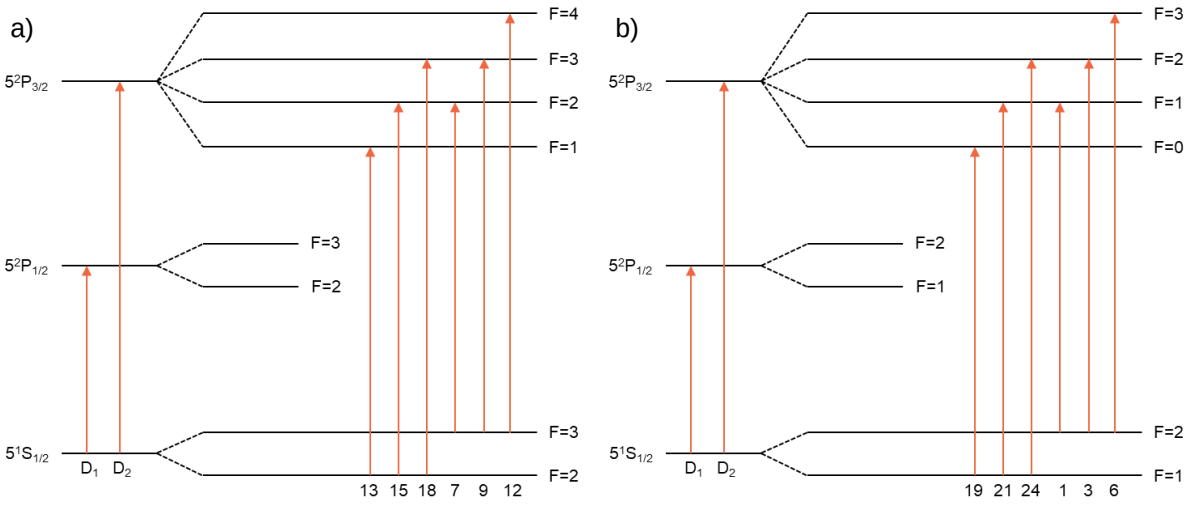

Fig. 5 Scheme for the hyperfine transitions in a) ^{85}Rb and b) ^{87}Rb. The numbers assigned to the transitions correspond to the observed absorption peaks in Fig. 6.

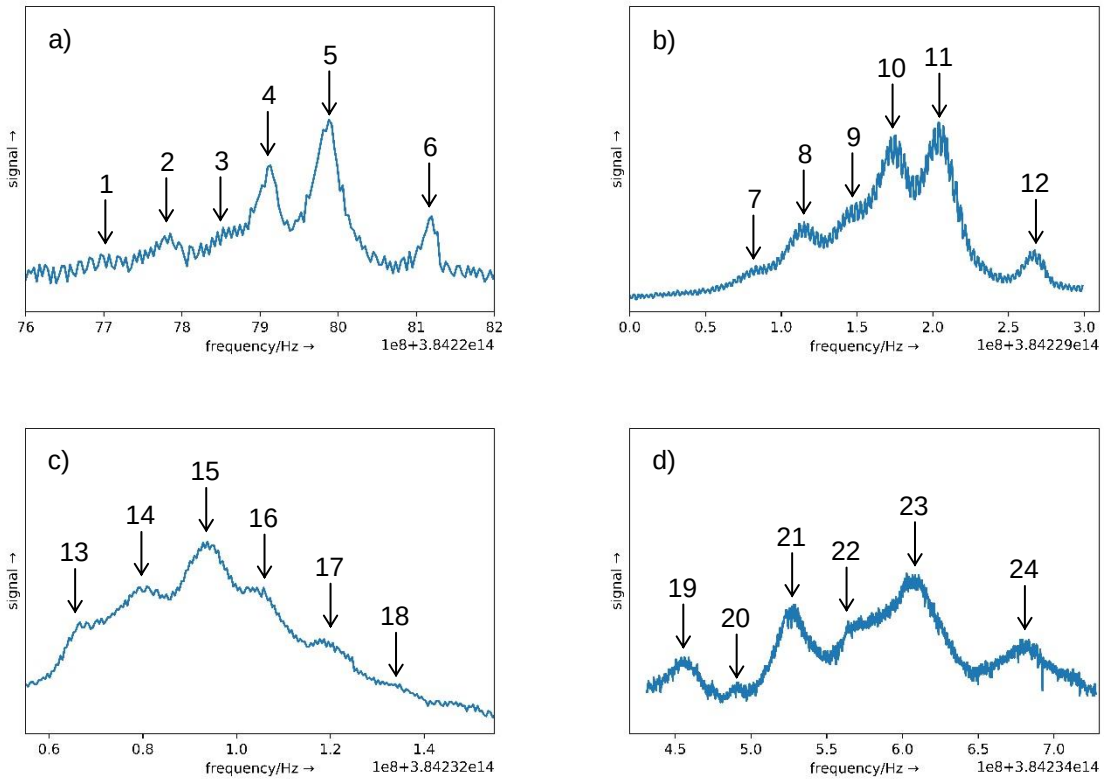

Fig. 6 Hyperfine transition and cross-over peaks in ^{85}Rb and ^{87}Rb. a) ^{87}Rb, F_i=2. **1** F_f=1. **2** Cross-over between F_f=1 and F_f=2. **3** F_f=2. **4** Cross-over between F_f=1 and F_f=3. **5** Cross-over between F_f=2 and F_f=3. **6** F_f=3. b) ^{85}Rb, F_i=3. **7** F_f=2. **8** Cross-over between F_f=2 and F_f=3. **9** F_f=3. **10** Cross-over between F_f=2 and F_f=4. **11** Cross-over between F_f=3 and F_f=4. **12** F_f=4.9 c) ^{85}Rb, F_i=2. **13** F_f=1. **14** Cross-over between F_f=1 and F_f=2. **15** F_f=2. **16** Cross-over between F_f=1 and F_f=3. **17** Cross-over between F_f=2 and F_f=3. **18** F_f=3. d) ^{87}Rb, F_i=1. **19** F_f=0. **20** Cross-over between F_f=0 and F_f=1. **21** F_f=1. **22** Cross-over between F_f=0 and F_f=2. **23** Cross-over between F_f=1 and F_f=2. **24** F_f=2.

The line width of the hyperfine transition and cross-over peaks is $18\text{MHz} \leq \Delta\nu \leq 27\text{MHz}$, an order of magnitude smaller than the Doppler-broadened peaks. The limit on decreasing the line width is set by the natural line width determined by the finite lifetime τ of the excited states which is linked by Heisenberg´s uncertainty principle to an uncertainty in the energy and frequency:

$$\Delta\nu_{\text{nat}} = \frac{\Delta E}{h} = \frac{1}{2\pi\tau}$$

The natural line width can therefore only be altered by changing the lifetime of the excited state. An exemplary lifetime of $\tau = 26.2348(77)\ \text{ns}$ [5] for the D_2-transitions in ^{85}Rb is followed by a natural line width of $\Delta\nu_{\text{nat}} = 6.0666(18)\text{MHz}$. The difference between this theoretical and the observed line width results from other broadening effects like collisions between atoms shortening the lifetime of the excited states.

3 Generation of the feedback signal

To generate the feedback signal as described in the introduction an acousto-optic modulator (AOM) is inserted in the path of the laser beam (Fig. 7). The desired modulation is added to the laser frequency by using the first-order beam from the light passed through the AOM with the frequency

$$\nu_f(t) = \nu_i(t) - \nu_{AOM}(t)$$

and applying a frequency modulated signal to the AOM which is produced by a function generator using the internally created reference from the lock-in amplifier as a modulation frequency and a carrier frequency of $\nu_{carr} = 90\text{MHz}$.

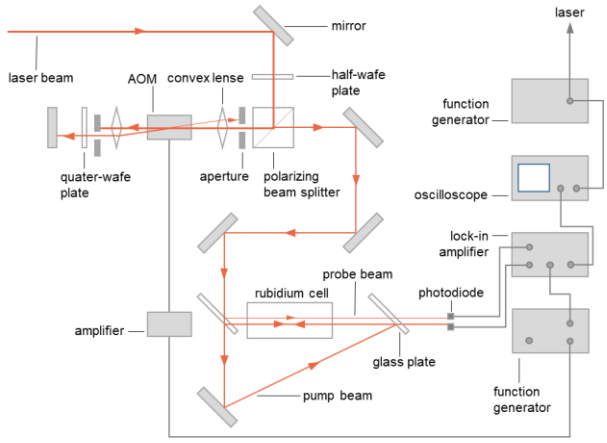

Fig. 7 Experimental setup to generate a feedback signal for the laser.

The obtained signal displays the expected peaks but is missing the distinct zero crossings as the narrow signals corresponding to the hyperfine and cross-over transitions are located in a larger broader peak related to the Doppler-broadened signal (Fig. 8).

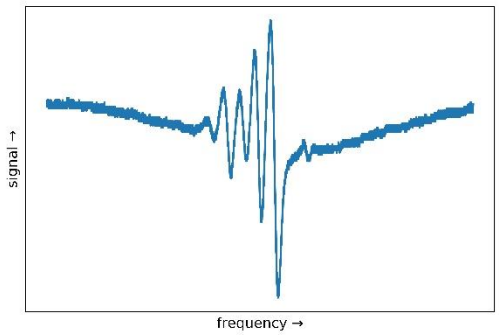

Fig. 8 Obtained feedback signal using the setup in Fig. 7.

4 Modified experimental setup

Modifying the setup in a way that only the pump beam is modulated in frequency instead of the probe and pump beams (Fig. 9) improves the form of the obtained error

signal (Fig. 10). Using an external frequency generator instead of the internal oscillator from the lock-in amplifier to produce the reference frequency for the lock-in amplifier solves the problem of the lock-in amplifier settings not allowing the reference frequency to be set to its internal oscillation frequency. In the previous setup this resulted in an unexpected sharp optimum for the modulation frequency, which should be adjustable over a broad range. Further improvements in the signal can be achieved by adjusting the integration time in the lock-in amplifier to several periods which filters arising interfering frequencies.

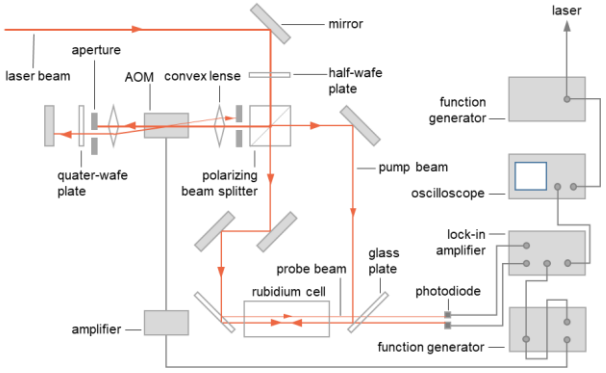

Fig. 9 Modified setup.

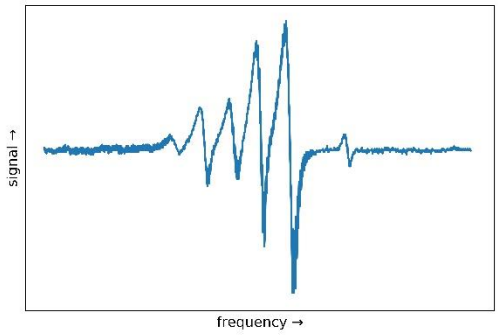

Fig. 10 Improved feedback signal using the setup in Fig. 9.

For the purpose of locking the laser to a hyperfine transition by decreasing the scanning range and using the error signal as a feedback to the control interface a switch box and a potentiometer were installed in the setup (Fig. 11).

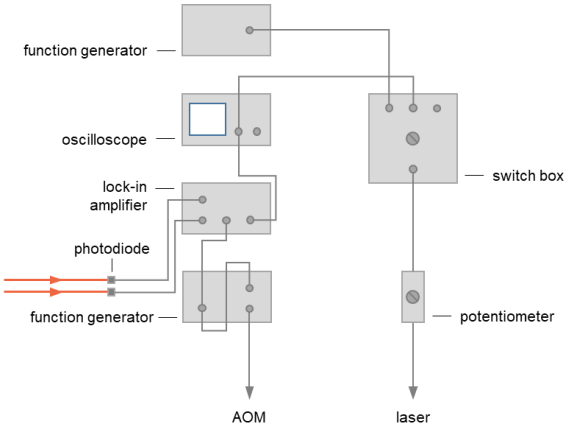

Fig. 11 Setup for locking the laser to a hyperfine transition.

Decreasing the scanning range by lowering the voltage of the ramping signal with the potentiometer revealed a noise signal in the lock-in amplifier output (Fig. 12 and Fig. 13) which impeded with locking the laser.

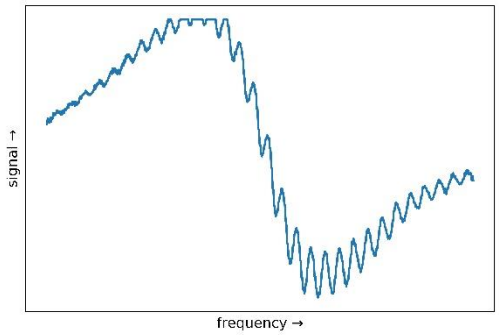

Fig. 12 A hyperfine transition in the error signal at a decreased frequency scanning range.

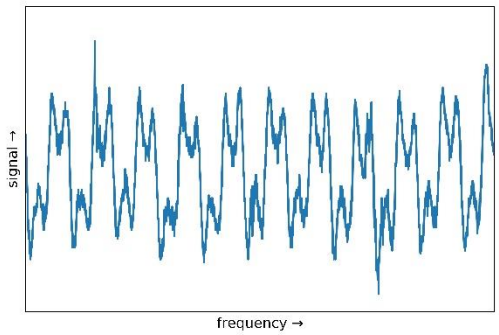

Fig. 13 The noise signal in the error signal, the scan is centred at a zero crossing and the scan amplitude is zeroed.

5 Troubleshooting

A fourier transform of the noise signal (Fig. 14) shows three main frequency components of $\nu_1 = 60\text{Hz}$, $\nu_2 = 120\text{Hz}$ and $\nu_3 = 180\text{Hz}$ which indicates interfering electrical systems connected to the mains frequency and voltage. Connecting all electrical components of the setup in pairs by a highly conductive copper band and therefore eliminating potential differences between them does not affect the signal.

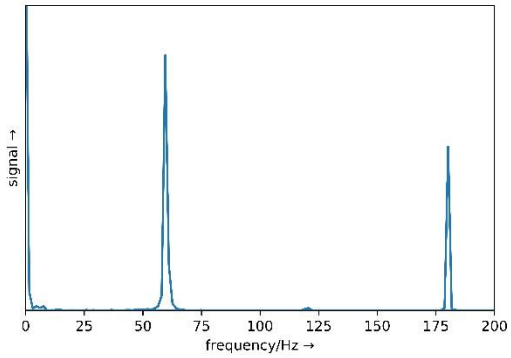

Fig. 14 Fourier transform of the noise signal in the error signal.

5.1 Surrounding conditions

Turning off the light and the ventilation in the laboratory does not show any effect on the signal.

5.2 Testing and exchanging components

Replacing the oscilloscope, the lock-in amplifier, the frequency generators used for generating the ramping voltage, the modulation frequency and the frequency modulated signal, the switch box, the potentiometer, the set of photodiodes and the amplifier prior to the AOM separately does not change the signal nor does exchanging each used BNC cable and Tee connector one at a time. The frequency modulated signal for the AOM is monitored by several fourier transforms and found to have the expected form, the maximum frequency deviation from the carrier frequency of $\nu_{\mathrm{carr}} = 90\mathrm{MHz}$ is $\nu_{\mathrm{def}} = 1.6\mathrm{MHz}$. The efficiency of the AOM varies with the applied frequency and therefore the intensity of the first-order beam changes which does not have any effect on the signal since the intensity difference is small due to the small-scale frequency deviations and while the signal does strongly correlate to the probe beam intensity the intensity of the pump beam is variable in a range including the deviations caused by the AOM without any changes.

5.3 Structural changes in the setup

In an attempt to separate the electrical circuits between the laser control interface and the other components of the setup an additional amplifier is installed between the potentiometer and the control interface which does not change the noise. Feeding the output from the lock-in amplifier through a PID controller does also not improve the signal.

5.4 Testing the laser

To eliminate the laser as a cause of the noise signal its light is overlapped with a beam from a structurally identical laser with a similar intensity and polarization and a close frequency. One of the two expected beating frequencies can be observed on the oscilloscope which changes as the frequency difference between the two slowly drifting lasers fluctuates, but no additional beating frequency indicating a noise signal on the laser light can be seen. The noise does not appear if not an external ramping voltage

but the internal cavity scan is used to ramp the laser frequency indicating the cause of the problem is not located in the laser.

5.5 Physical Effects

The noise signal appears in all hyperfine transition and cross-over peaks of the D_2- as well as the D_1-transitions for ^{85}Rb and ^{87}Rb. Shielding the rubidium tube with Mu-metal results in a small decrease in the amplitude of the noise signal, however examining the area around the rubidium cell with a Hall probe for magnetic fields does not lead to noticeable results. The polarisation of the laser light can be changed by inserting waveplates in the beam path. As long as probe and pump beams have the same polarisation an error signal with noise can be detected, whereat the form of the error signal but not the noise signal changes slightly with the polarisation due to different absorption because of the surrounding magnetic field. When the rubidium cell is placed inside a copper coil with an applied current the resulting magnetic field leads to a separation of electron energy levels because the magnetic dipole moments of the electrons interact with the external magnetic field (Zeeman effect). [2] This results in a change of the absorbed frequencies for the hyperfine transitions and a distinctively different absorption spectrum is obtained by setting the laser to a fixed frequency and applying an oscillating current to the coil causing the absorption frequencies to change. The noise signal can be found in this absorption signal as well.

5.6 Final results

The setup is changed in a way that all electrical components are connected to the same power supply, isolated from the laboratory tables and the laboratory tables are connected to ensure a common ground for all electrical devises. This does not eliminate the signal, which seems to only disappear when the laser control interface is disconnected from the other electrical components.

6 Summary and outlook

Saturation spectroscopy allows the observation and identification of hyperfine transitions and related cross-over peaks of the two natural rubidium isotopes ^{85}Rb and ^{87}Rb in the Doppler-broadened absorption peaks. Using an additional frequency modulation and a lock-in amplifier a feedback signal can be produced that might be used to stabilise the laser on a hyperfine transition which is currently prevented by a 60Hz noise signal. Once the laser is locked to a fixed frequency the scanning Fabry-Perot cavity and the Python program normally used to lock the Ti:Sap laser to the HeNe laser can be used to observe the absorption peaks of the HeNe laser relative to the stable Ti:Sap laser resulting in an evaluation of the stability of the HeNe laser which is the critical value in stabilising the Ti:Sap laser for the collinear laser spectroscopy experiment.

7 References

[1] A. Voss, T.J. Procter et al.: The Collinear Fast Beam laser Spectroscopy (CFBS) experiment at TRIUMF. Nuclear Instruments and Methods in Physics Research A, 811, 2016, p. 57–69.

[2] M. Oberthaler: Der Spin des Elektrons. Unpublished lecture notes, Heidelberg, 2018, p. 11-16.

[3] F. Mooshammer: Laser Spectroscopy at TRIUMF. 2014, p. 21-24.

[4] M. Weel, A. Kumarakrishnan: Laser-frequency stabilization using a lock-in amplifier. Canadian Journal of Physics, 80, 2002, p.1449–1458.

[5] D.Steck: Rubidium 85 D Line Data. Online at http://steck.us/alkalidata (access: 17.08.2019), 2010, p. 17-25.

[6] D.Steck: Rubidium 87 D Line Data. Online at http://steck.us/alkalidata (access: 17.08.2019), 2003, p. 23.